# LOG ANALYSIS AND INTEGRATION WITH CORE DATA

A Report by ODIN Reservoir Consultants

DMIRS/2018/2




December 2017

Mike Walker

Government of **Western Australia**
Department of **Mines, Industry Regulation and Safety**

**1. EXECUTIVE SUMMARY ..... 4**

**2. INTRODUCTION ..... 5**

**3. LOG ANALYSIS AND INTEGRATION WITH CORE DATA ..... 10**

3.1 REVIEW OF CURRENT LOG ANALYSIS ..... 10
3.2 REVIEW OF SPECTRAL GAMMA RAY ..... 10
3.3 REVIEW OF POROSITY DEPTH TREND USING OFFSET WELLS ..... 11
3.4 REVIEW OF NUCLEAR MAGNETIC RESONANCE ..... 12
3.5 ASSESS PERMEABILITY TO AIR AND BRINE (KAIR, KBRIN RATIOS) ..... 12
3.6 UPDATE POROSITY TO PERMEABILITY RELATIONSHIPS ..... 14
3.7 REVIEW IMAGE LOG ANALYSIS AND INTEGRATED WITH SEISMIC ..... 19
3.8 ANALYSIS OF SEAL QUALITY ..... 23
3.9 EVALUATION OF PALEOSOL OCCURRENCE ..... 25
3.10 ASSESS ALL AVAILABLE DATA ON THE WONNERUP ..... 29

**4. REFERENCES ..... 32**

**List of Figures**

Figure 2-1: Harvey Location Map ..... 5
Figure 2-2“Break-up" Event (After Reference 1) ..... 8
Figure 2-3 Late Triassic Climate (After Reference 3) ..... 8
Figure 2-4 Stratigraphy of Perth Basin (Harvey Area within red box). (After Reference 2.) ..... 9
Figure 3-1: Location Map of Offset Wells. ..... 11
Figure 3-2: Cross plot of Permeability: Air to Brine ..... 14
Figure 3-3: 2016 Wonnerup Porosity - Permeability Transform ..... 15
Figure 3-4: 2016 Yalgorup Porosity - Permeability Transform ..... 15
Figure 3-5: Wonnerup Log Derived Total Porosity vs NMR Perm ..... 16
Figure 3-6: Revised Porosity Permeability Transform for Wonnerup ..... 17
Figure 3-7: Yalgorup Porosity vs Permeability NMR (Left) & Core (Right) ..... 17
Figure 3-8: Yalgorup Porosity Permeability Transform ..... 18
Figure 3-9: Porosity Permeability By Facies ..... 19
Figure 3-10: GSWA Harvey 1 Composite Log showing Fractures from Image Log ..... 21
Figure 3-11: GSWA Harvey 1 Overview of Fractures from Baker Hughes Image Log Study ..... 22
Figure 3-12: DMP Harvey 2 Composite Log showing Fractures Estimated from Core ..... 22
Figure 3-13: DMP Harvey 4 Composite Log showing Fractures from Image Log ..... 23
Figure 3-14: Geomechanical & MICP Data from GSWA Harvey 1 ..... 24
Figure 3-15: DMP Harvey 4 NMR T2 spectra showing abundant micropores ..... 25
Figure 3-16: GSWA Harvey 1 Spectral Gamma Ray ..... 27
Figure 3-17: SEM-EDS data ..... 28
Figure 3-18: Higher Porosity in lower Wonnerup Member (GSWA Harvey 1, Lake Preston 1, and Sabina River 1) ..... 30
Figure 3-19: Higher Porosity in lower Wonnerup Member (Pinjarra 1, Wonnerup 1 & Whicher Range 4) ..... 31

## *Declaration*

*ODIN Reservoir Consultants was commissioned to undertake to provide a reservoir modelling study for the South West Hub $CO_2$ Sequestration Project on Department of Mines, Industry Regulation and Safety, (DMIRS).*

*The evaluation of Carbon Capture and Storage is subject to uncertainty because it involves judgments on many variables that cannot be precisely assessed, including $CO_2$ sequestration rates and capture, the costs associated with storing these volumes, sequestration gas distribution and potential impact of fiscal/regulatory changes.*

*The statements and opinions attributable to us are given in good faith and in the belief that such statements are neither false nor misleading. In carrying out our tasks, we have considered and relied upon information supplied by the DMIRS and available in the public domain. Whilst every effort has been made to verify data and resolve apparent inconsistencies, neither ODIN Reservoir Consultants nor its servants accept any liability for its accuracy, nor do we warrant that our enquiries have revealed all of the matters, which an extensive examination should disclose.*

*We believe our review and conclusions are sound but no warranty of accuracy or reliability is given to our conclusions.*

*Neither ODIN Reservoir Consultants nor its employees has any pecuniary interest or other interest in the assets evaluated other than to the extent of the professional fees receivable for the preparation of this report*

**Note:**

*ODIN has conducted the attached independent technical evaluation with the following internationally recognised specialist:*

*Mike Walker is an expert in the petrophysical evaluation of reservoirs, as well as experienced in the planning and evaluation of exploration and development drilling programmes. The evaluations covered all aspects of petrophysics within different types of reservoirs, hydrocarbons and drilling fluids. Mike has experience in exploration and production geology, economic assessment and prospect ranking through risking and basin analysis. He is also experienced with tools, data and products from the major wireline and FEWD logging companies. He was the founding President of the Formation Evaluation Society of Victoria, a chapter of the Society of Petrophysicists and Well Log Analysts.*

# 1. EXECUTIVE SUMMARY

The Harvey structure, onshore southern Perth Basin, is a North-South elongated fault bounded anticline. The study area for this project within this structure covers 332 $km^2$ and is located approximately 13km northwest of the town of Harvey south of Perth.

ODIN Reservoir Consultants was commissioned by the Department of Mines, Industry Regulation and Safety (DMIRS) to provide a multi-disciplinary group with sub-surface skill sets to:

i. provide modelling and interpretation support to update the existing models by considering additional data such as infill seismic, new core analysis etc. to reduce the uncertainties identified in the Uncertainty Management Plan (UMP) and test the results against defined criteria; and
ii. update the current Uncertainty Management Plan (UMP) and provide uncertainty reduction options through new data acquisition.

Several “work-streams” have been defined as the work scope for this phase of the project:

- Work-stream 1: Advanced Seismic Processing (Provided by Curtin)
- Work-stream 2: Advanced Seismic Interpretation
- Work-stream 3: Log Analysis and integration with Core Data
- Work-stream 4: Geomechanics Update and Integration
- Work-stream 5: Geology Update and Integration
- Work-stream 6: Engineering Update and Integration
- Work-stream 7: Static Modelling
- Work-stream 8: Dynamic Modelling
- Work-stream 9: UMP update, Injectivity and Capacity Expectation Curves

Work-streams 7-9 will proceed upon completion of Phase 1 (Work-streams 1 to 6) which has resulted in building a table of various reservoir and fluid parameters resulting in a probabilistic evaluation of injection rates and capacities and POS computations for injectivity and containment using simulation models and analytical approaches.

## 2. INTRODUCTION

The Harvey structure (Figure 2.1) in the southern Perth Basin, which covers an approximate area of 332km$^2$, constitutes a potential storage area for $CO_2$ sequestration. The sandstone rich Wonnerup Member in the Lesueur Formation forms the target injection reservoir, with the containment (based on previous studies) within the same sands of the Wonnerup Member. However, the overlying Yalgorup member, which is represented by the paleosol rich, will be assessed in greater detail to reveal its containment potential should the plume migrate vertically into this member.

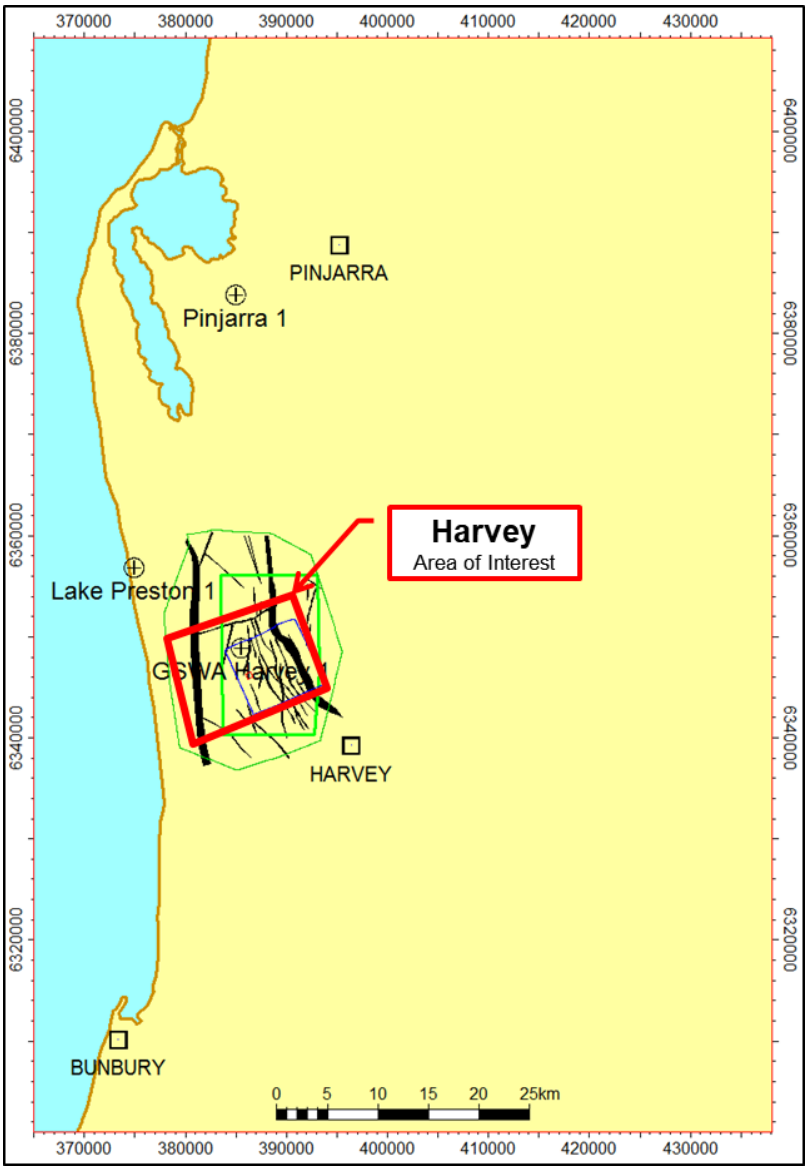



**Figure 2.1: Harvey Location Map**

Log analysis is the interpretation of the logs acquired in each well and forms the basis for “Data Analysis” (Figure 2.2) which is used as input into the “Petrophysical Modelling” stage. Log analysis defines the ranges of properties observed in the wells and highlights trends or relationships between the properties and wells drilled. This may result in defining areal or vertical trends and possibly a rock type or facies association.

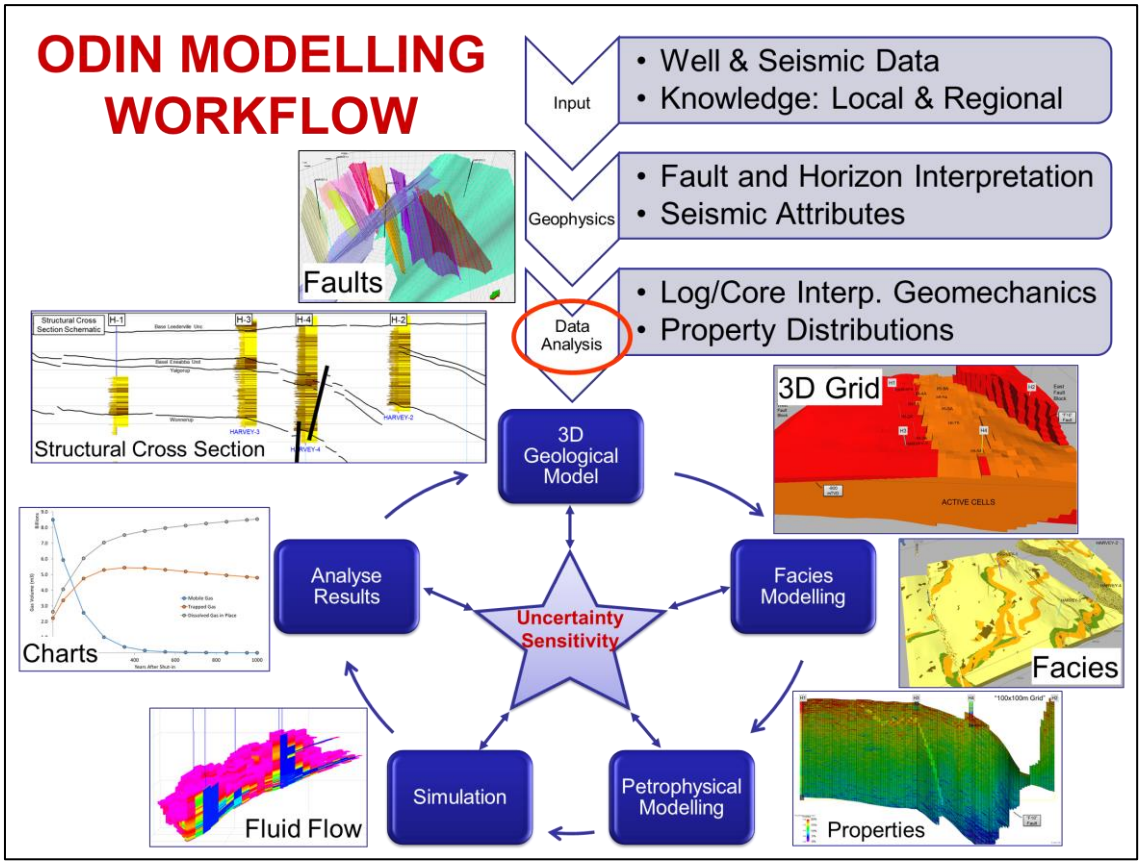



**Figure 2.2: ODIN Modelling Workflow**

The Lesueur Formation was developed in the southern Perth Basin during the Late Triassic (Figure 2.3 and Figure 2.5). At that time, the basin was undergoing a phase of thermal subsidence as a result of an initial stage of rifting in the Gondwana supercontinent. This rifting event took place from the late Permian to the Lower Cretaceous when the final break-up of the continent occurred, and the drifting phase of India/Australia began (Figure 2.3)

During the Late Triassic, the global climate was generally warm; there was no ice at either North or South Poles and warm temperate condition extended to the poles. The Perth Basin region was under a warm temperate regime (Figure 2.4).

The Lesueur formation was deposited in a braided fluvial environment. The paleogeography of the basin indicates an elongated shape roughly running in a North-South direction and bounded by stable cratons, which constitute the sediment source.

The exact provenance of the Perth Basin sediments is still an open question but according to mineralogical analysis is likely to come from stable cratons and transitional continents such as Yilgarn craton, Leeuwin complex or Albany-Fraser orogeny, or any combination of these three sources. The main sediment supply direction has been identified as a general West-East trend with a certain West South West-East North East component.

Five main depositional facies spreading from channel fill sands to swampy overbank deposits and paleosol/floodplain sediments have been defined to represent both fluvial environments, braided and meandering, in the Wonnerup and Yalgorup respectively. The two lithostratigraphic members that comprise the Lesueur Formation, Wonnerup Member and Yalgorup Member present some depositional differences. The Wonnerup Member is formed by a fluvial braided system dominated by linguoid bars whereas the Yalgorup Member is formed by a fluvial meandering system dominated by point bars, claystone irregular bodies and paleosol's.

In general, the coarse channel fill sands in the Wonnerup Member are a good reservoir to contain the injected $CO_2$ and the more clay rich Yalgorup Member dominated by floodplain and paleosols deposits can act as a seal for the reservoir complex. The present analogue used for both fluvial systems in the Wonnerup and Yalgorup Members is the Brahmaputra braided river. This example constitutes a good guide to design the modelling parameters of the reservoir formation.

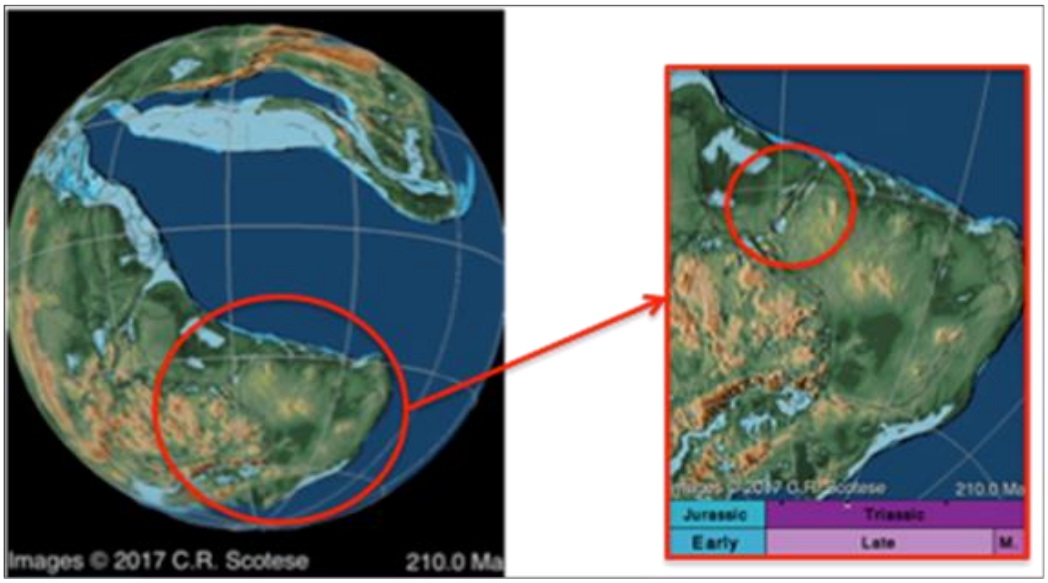



**Figure 2.3“Break-up" Event (After Reference 1)**

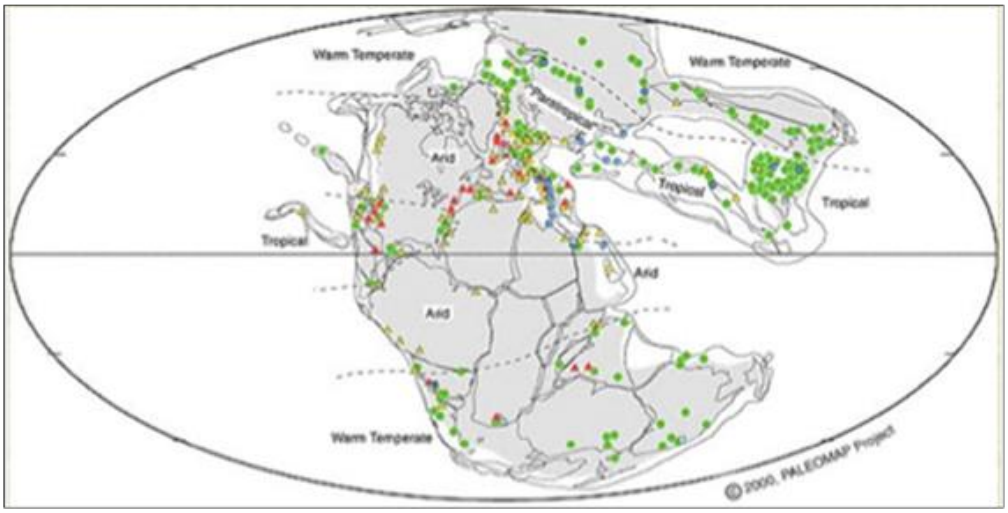



**Figure 2.4 Late Triassic Climate (After Reference 3)**

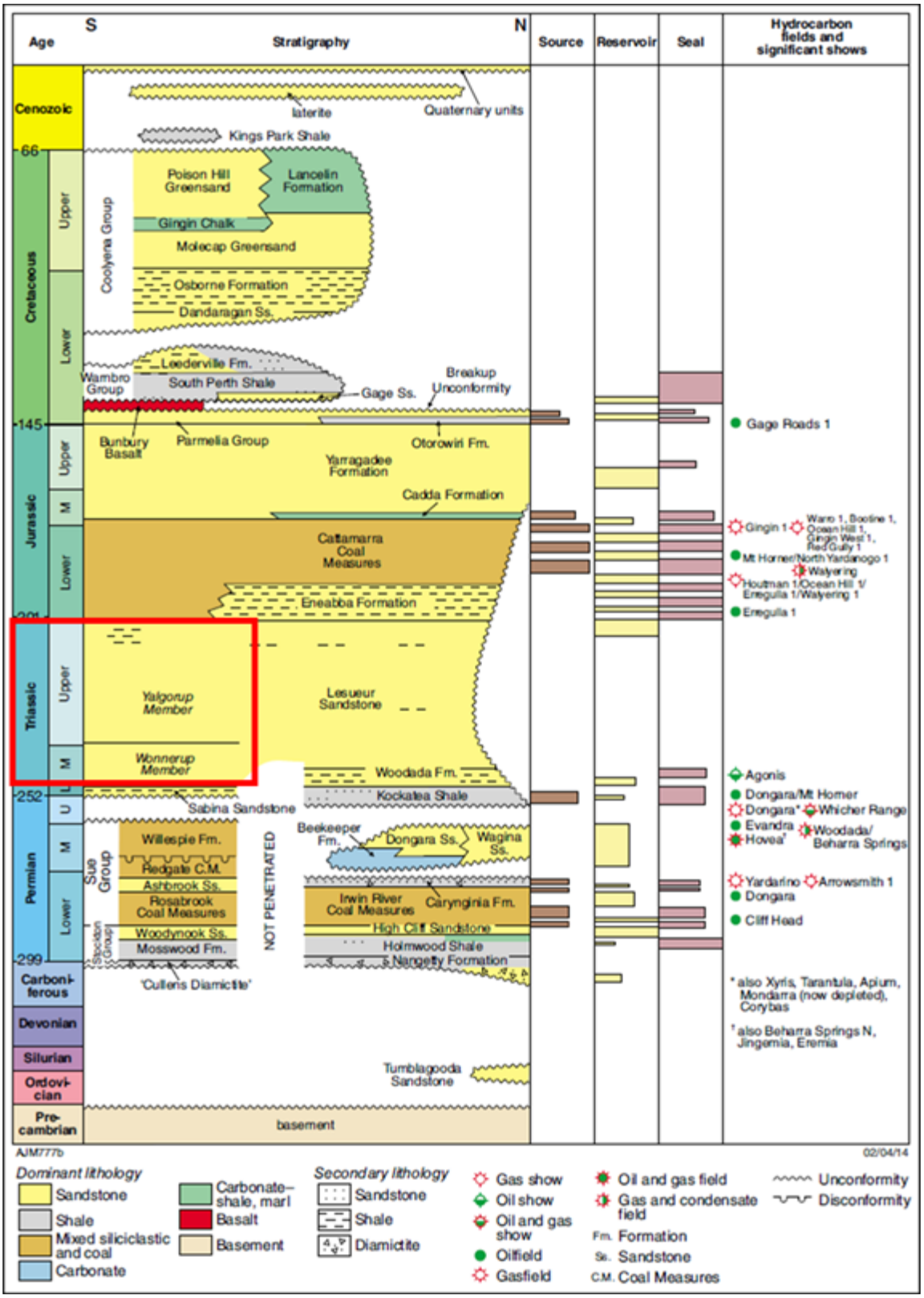



**Figure 2.5 Stratigraphy of Perth Basin (Harvey Area within red box). (After Reference 2.)**

# 3. LOG ANALYSIS AND INTEGRATION WITH CORE DATA

## 3.1 Review of current log Analysis

The original petrophysical analysis undertaken on the four (4) Harvey wells was reviewed. GSWA Harvey 1 included a reasonably rich wireline log data set with the exception of limited NMR coverage. GSWA Harvey 1 was the only well in the current programme to penetrate the entire Wonnerup member. The data sets for DMP Harvey 2 and DMP Harvey 3 were limited with DMP Harvey 2 possessing only an acoustic transit time measurement for porosity determination, and the data set for DMP Harvey 4 was comprehensive including Nuclear Magnetic Resonance (NMR) over the section of Wonnerup member penetrated as well as the entire Yalgorup member and most of the Eneabba Formation. The well data set also contains and good amount of whole core and a good spread of conventional core analysis.

Only GSWA Harvey 1 and DMP Harvey 4 were logged with a spectral Gamma ray too, which breaks the gamma spectrum into components associated with Potassium, Thorium and Uranium. It would be possible to log the available core from DMP Harvey 2 and DMP Harvey 3 with a spectral detector and augment the data set and if possible the core from GSWA Harvey 1 and DMP Harvey 4 to provide comparison data.

The interpretations carried out during previous analysis are adequate given the data acquired:

- Porosity was well characterised
- However, the permeability transforms need revision (see subsequent section 3.6)

## 3.2 Review of Spectral Gamma Ray

During a meeting on 6 September 2017, it was discussed that determining shale fraction from the total Gamma Ray (GR) may lead to a pessimistic interpretation of shale layers in the Wonnerup Member. It was suggested that the increase in total GR was due to radioactive silt sized particle and not clay layers as noted by increases in the Thorium concentration independent of the Potassium concentration and that the Wonnerup Member was essentially 100% net porous reservoir. This effect of high gamma ray layers in sandstone is noted in many of the reservoirs of the southern Perth Basin where detrital

radioactive minerals may be found at the base of channels and other regions where heavy minerals can congregate.

It would have been useful to have recorded spectral Gamma Ray data in each well and to log the core with a spectral gamma ray device to enable the shale layers to be separated from lag deposits. This would also allow the correlation of the responses to the core to reduce the uncertainty in the interpretation over non-cored sections.

## 3.3 Review of Porosity Depth Trend using offset wells

The offset wells Pinjarra 1, Lake Preston 1, Sabina River 1, Wonnerup 1 and Whicher Range 4 were examined, for trends in porosity with depth, see (Figure 3.1). Only two wells (Lake Preston 1 and Whicher Range 4) had density data over the Lesueur Formation, with the other wells only having compressional slowness data (DT). The density coverage at Whicher Ranger 4 only extended over the bottom 500m of the ~1250m thick Wonnerup Member.

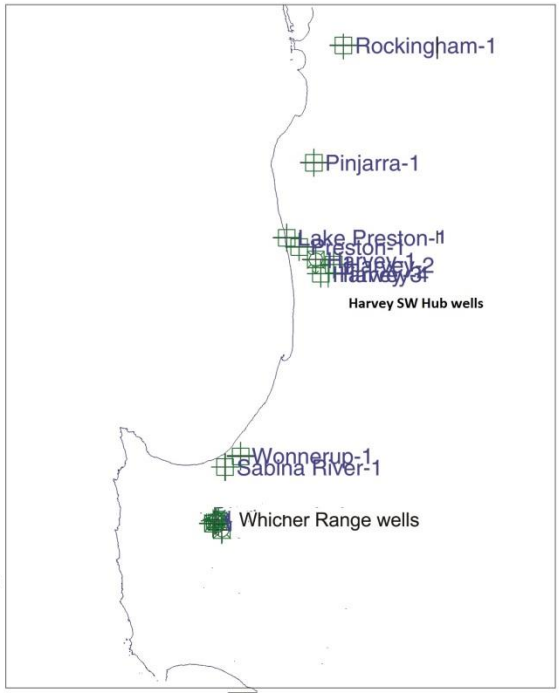



**Figure 3.1: Location Map of Offset Wells.**

## 3.4 Review of Nuclear Magnetic Resonance

Nuclear Magnetic Resonance (NMR) data has the potential to provide good quality information examining the pore systems of the intervals logged. The trade-off is that most NMR tools have poor vertical resolution, in the order of 1m, due to the physics of the measurement. The raw data is of little use to most and the standard processing carried out by the service companies focusses on determining the characteristics of conventional clastic reservoirs, which is the case at the SW Hub and given that, there is no hydrocarbon to complicate the response the standard processing is appropriate.

GSWA Harvey 1 and DMP Harvey 4 were logged with mandrel type NMR tools, which have an investigated volume the shape of a cylinder about 2mm thick and 1m high with a diameter of about 300mm from the centre of the well bore

GSWA Harvey 1 was logged, with the Baker Atlas MREX tool, which is one of the most recent NMR tools and incorporates some technology to improve the vertical resolution and increase the logging speed. The data acquired was in sections of the Wonnerup member and did not cover the Yalgorup member. DMP Harvey 4 was logged with the Halliburton MRIL tool, an older generation tool. Data was acquired over the upper Wonnerup member, Yalgorup member and Eneabba.

Both data sets appear to be of good quality. Both sets of data were processed by the respective service companies to the default wellsite/post-processing products, and this processing is considered adequate for the purposes of this project. It is felt that reprocessing the NMR data may improve the results marginally. It should be noted that specialised software is required, and the service companies who acquire the data would probably be best to do the processing. It is not felt that incurring additional costs of reprocessing the NMR data would add any value to the project.

## 3.5 Assess Permeability to Air and Brine (Kair, Kbrin ratios)

It is noted during a previous review that the Air and Brine permeability measurements exhibited a significant degree of scatter. The data were plotted on a log-log scale cross plot (Figure 3.2). It may be seen from the cross plot that the well with the most scatter is GSWA Harvey 1 (red squares) followed by DMP Harvey 3 (green triangles).

Geotek, supplied the GSWA Harvey 1 data with brine permeability values being derived from the Mercury Injection Capillary Pressure (MICP) data using the Swanson calculation (Swanson, 1981). It shows that this method does not work well at low permeability values (Reference 3) which appears to be the case with the GSWA Harvey 1 results.

Corelab using brine injection measured data for the other wells. This process resulted in the failure of many low permeability samples, and the results show considerable scatter. Whilst it may have been prudent from a data collection perspective to include low (less than 1md samples) in this study, realistically the low permeability component of the reservoir will not be involved in the sequestration process to the same degree as the more permeable reservoir.

There is noticeable increase in difference between air and brine as the permeability decreases using both methods in the region between 5 and 1000md there is reasonable agreement between the two methods.

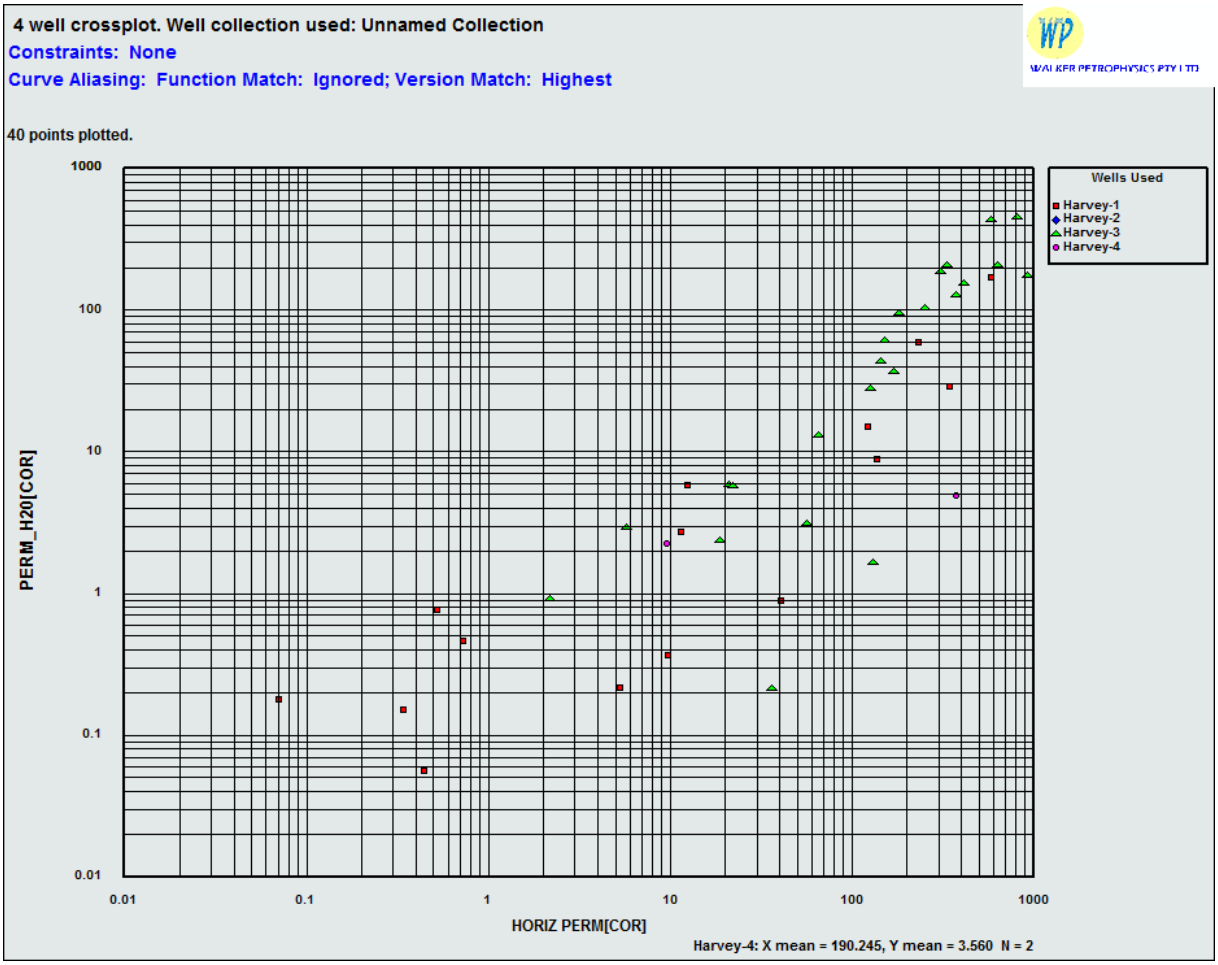



**Figure 3.2: Cross plot of Permeability: Air to Brine**

## 3.6 Update Porosity to Permeability relationships

Figure 3.3 and Figure 3.4 show the basic porosity to permeability transforms from the previous work. These transforms were derived from core data alone and it was felt that the NMR derived permeability would provide a richer data source and the transforms should be revised. It is noted that the concepts of using simple porosity to permeability transforms are essentially redundant when static reservoir models are employed to provide the reservoir property framework for the dynamic model. It is more appropriate to characterise the reservoir properties using the modelled geology, than to incorporate averaged properties derived from the well alone into the dynamic model.

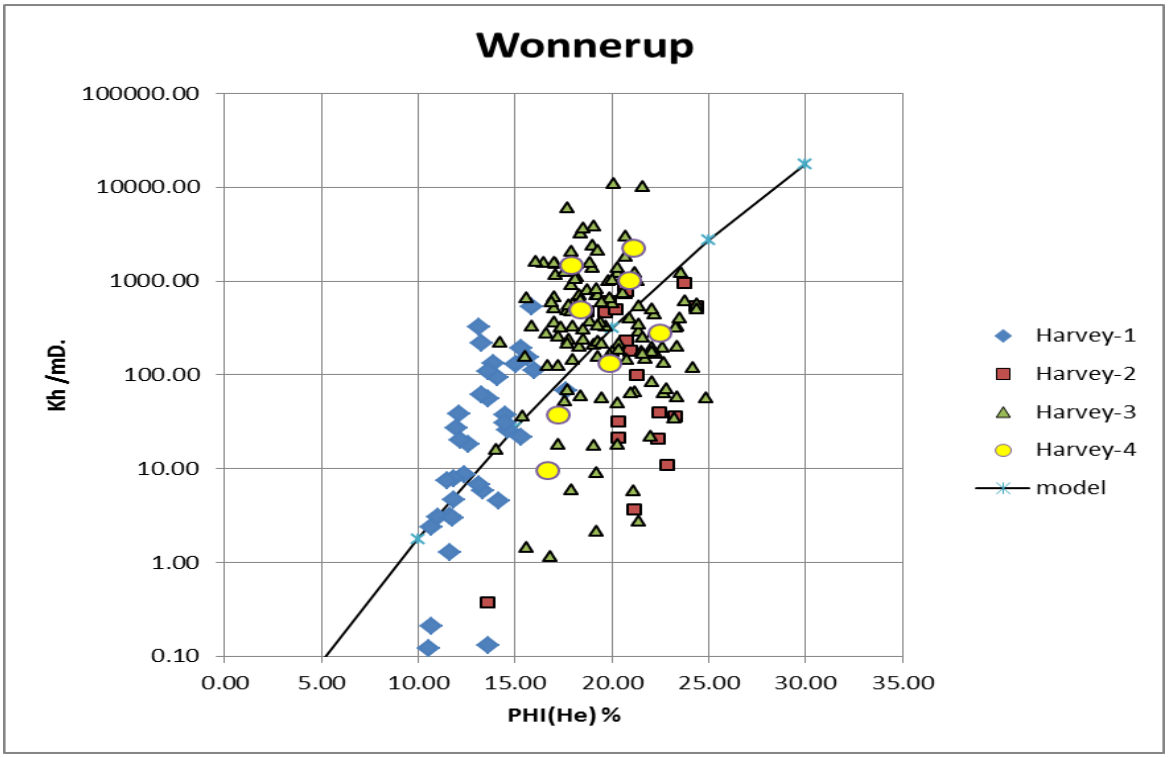



**Figure 3.3: 2016 Wonnerup Porosity - Permeability Transform**

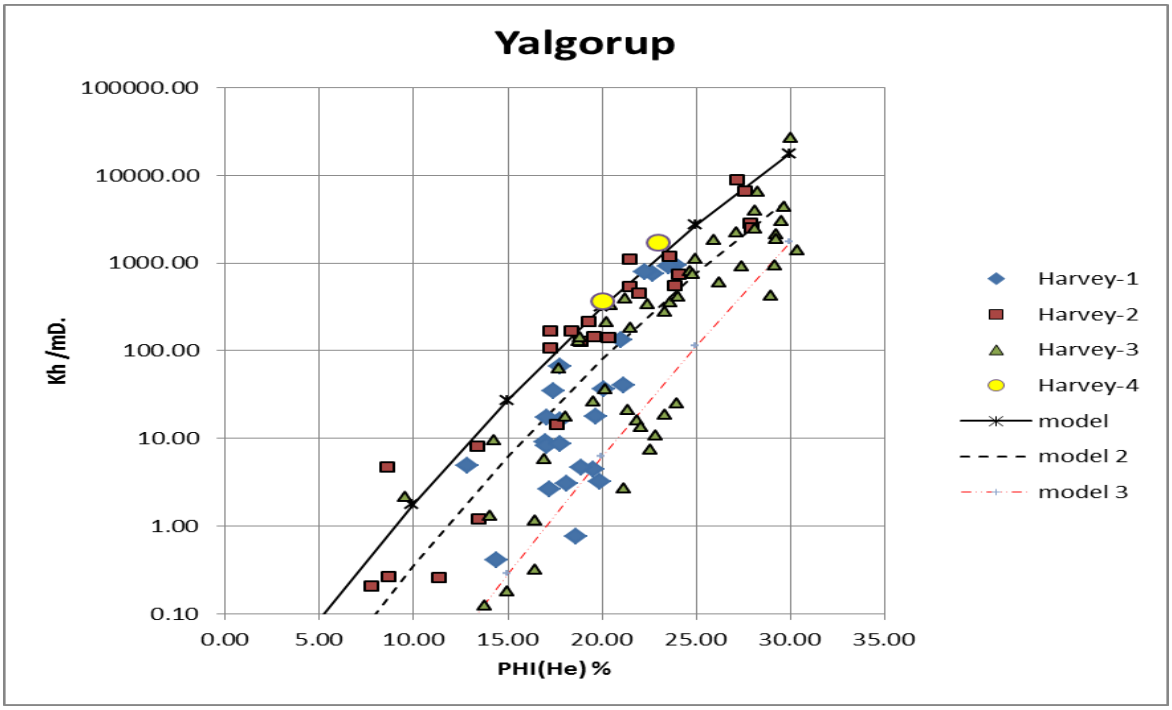



**Figure 3.4: 2016 Yalgorup Porosity - Permeability Transform**

The same mathematical approach was used, this being a second order polynomial.

$K = 10 ** (A + B\phi + C\phi^2)$

Log derived total porosity was plotted against the NMR derived permeability

Figure 3.5 and Figure 3.6 show data from GSWA Harvey 1 and DMP Harvey 4. Figure 3.7 shows the NMR data from the Yalgorup member from DMP Harvey 4. Figure 3.8 shows the core data.

Laying polygons around the core of the data allow the extraction of the following polynomials, which is an improvement on the previous transforms.

$K = 10**(32.8 * \phi - 51.1 * \phi^2 – 1.9)$ was derived for the Wonnerup

$K = 10**(12.8 * \phi + 30.8 * \phi^2 – 3.2)$ was derived for the Yalgorup

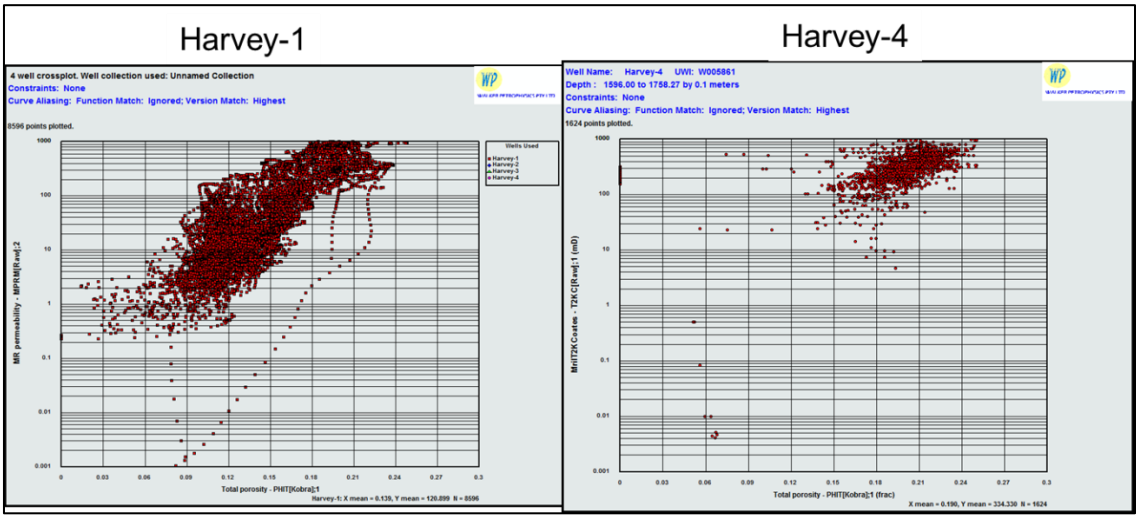



**Figure 3.5: Wonnerup Log Derived Total Porosity vs NMR Perm**

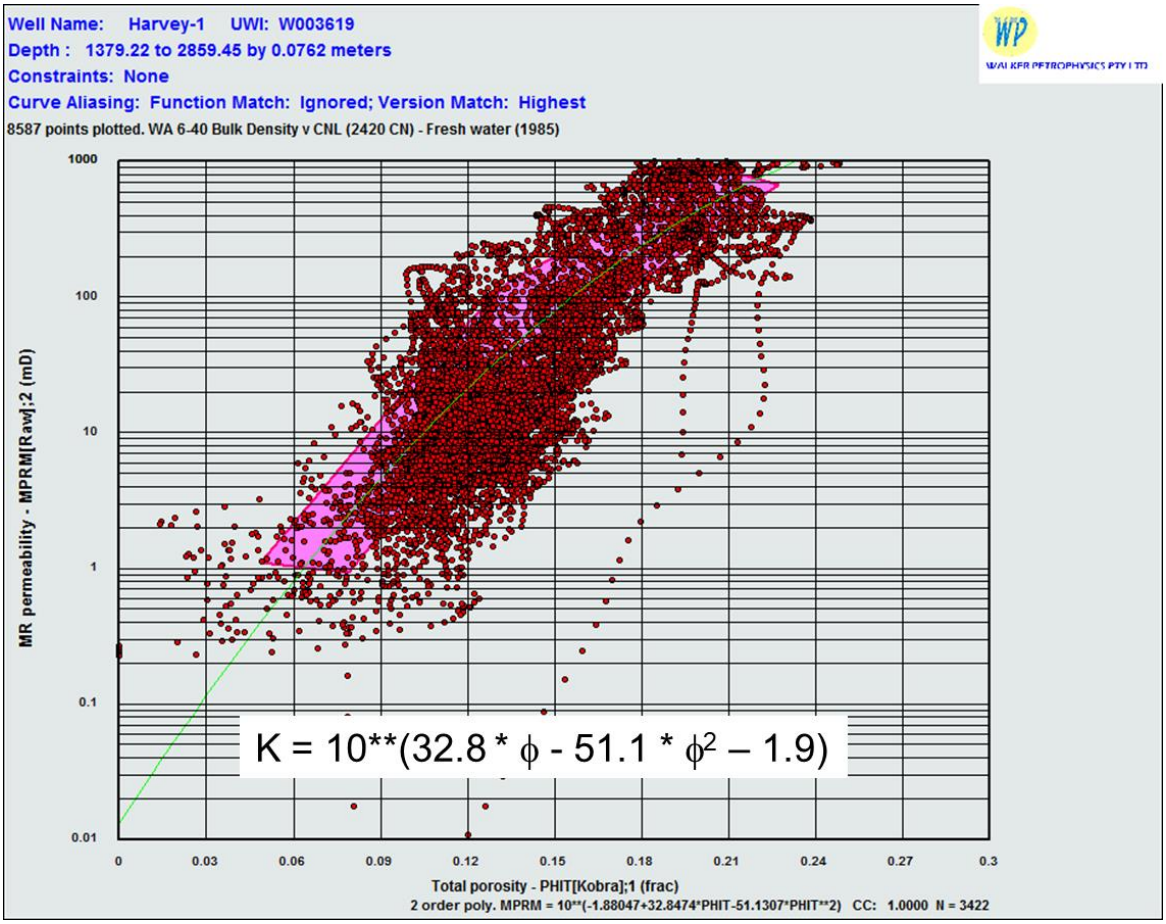



**Figure 3.6: Revised Porosity Permeability Transform for Wonnerup**

Harvey-4 Harvey-1,2,3,4 core

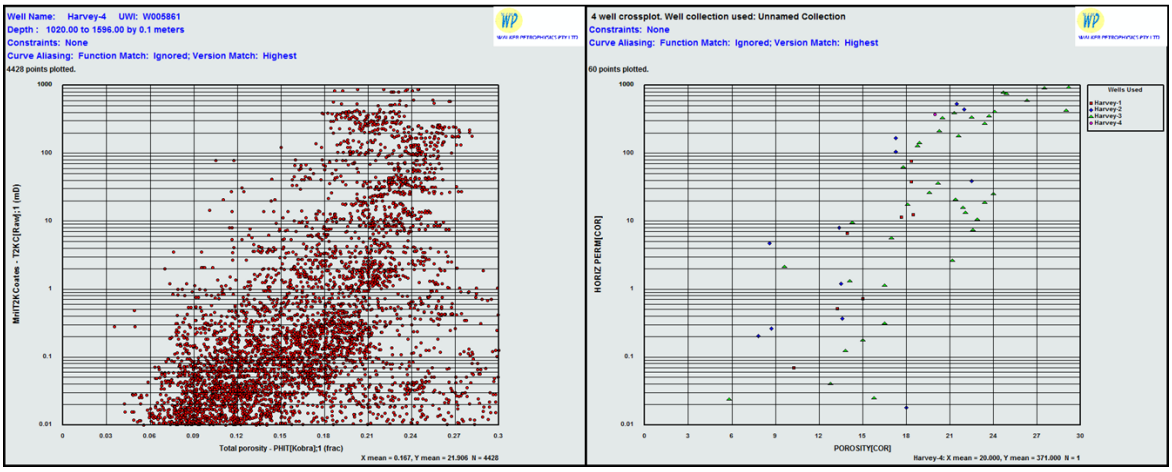



**Figure 3.7: Yalgorup Porosity vs Permeability NMR (Left) & Core (Right)**

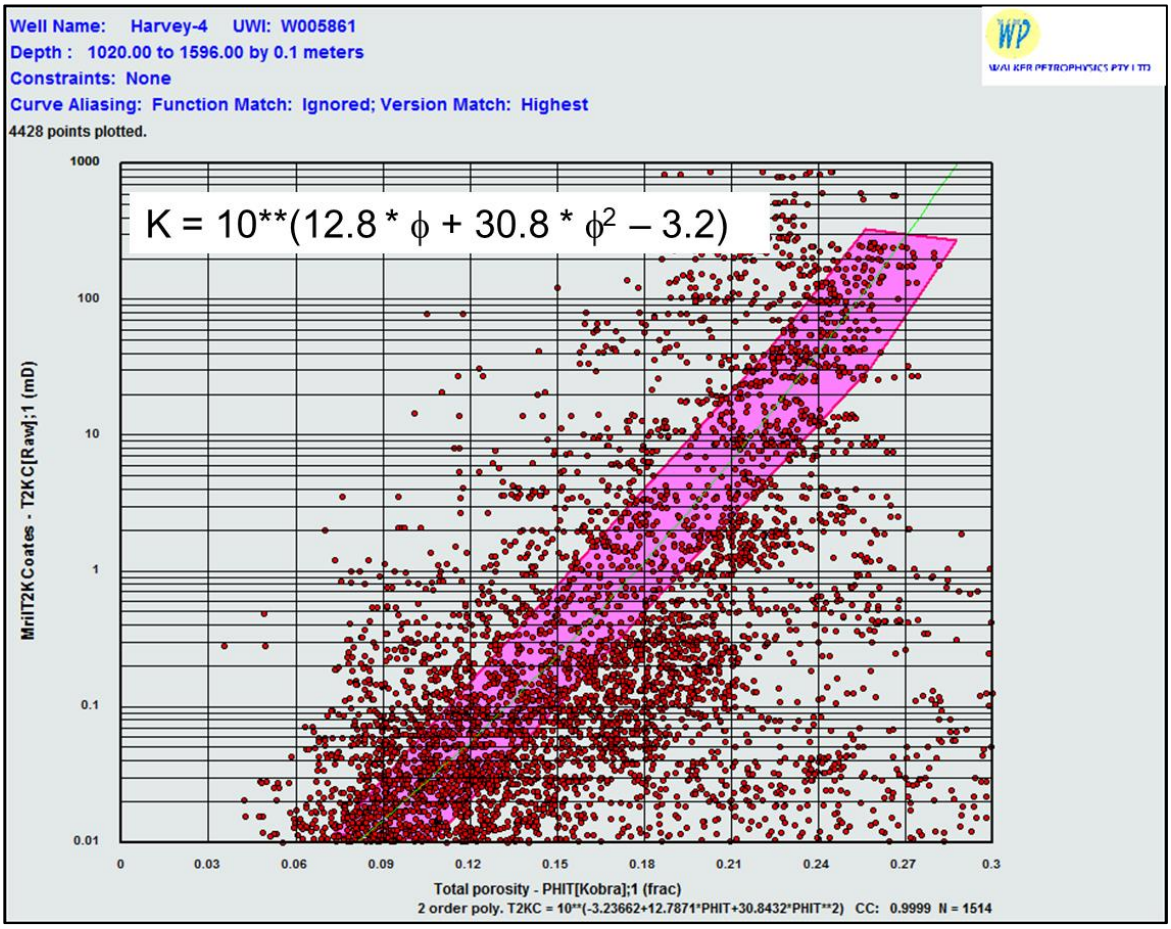



**Figure 3.8: Yalgorup Porosity Permeability Transform**

The observation of trends of porosity variation with depth, discussed in Section 3.3 and the departure from these trends in regional wells shows the product of the region's geological history. Since deposition, the Lesueur Sandstone has been transformed by burial, uplift, and diagenetic alteration of minerals. Porosity and permeability have been reduced and possibly enhanced in some places. It should be remembered that with only one penetration of the full Wonnerup section at the SW Hub the uncertainty on the reservoir parameters in the deeper section would remain significant.

Using the interpreted facies to drive the estimation of permeability in the static model is preferred over a reliance on simple 1D cross-plots. Figure 3.9 shows the porosity and permeability relationship's coloured by facies.

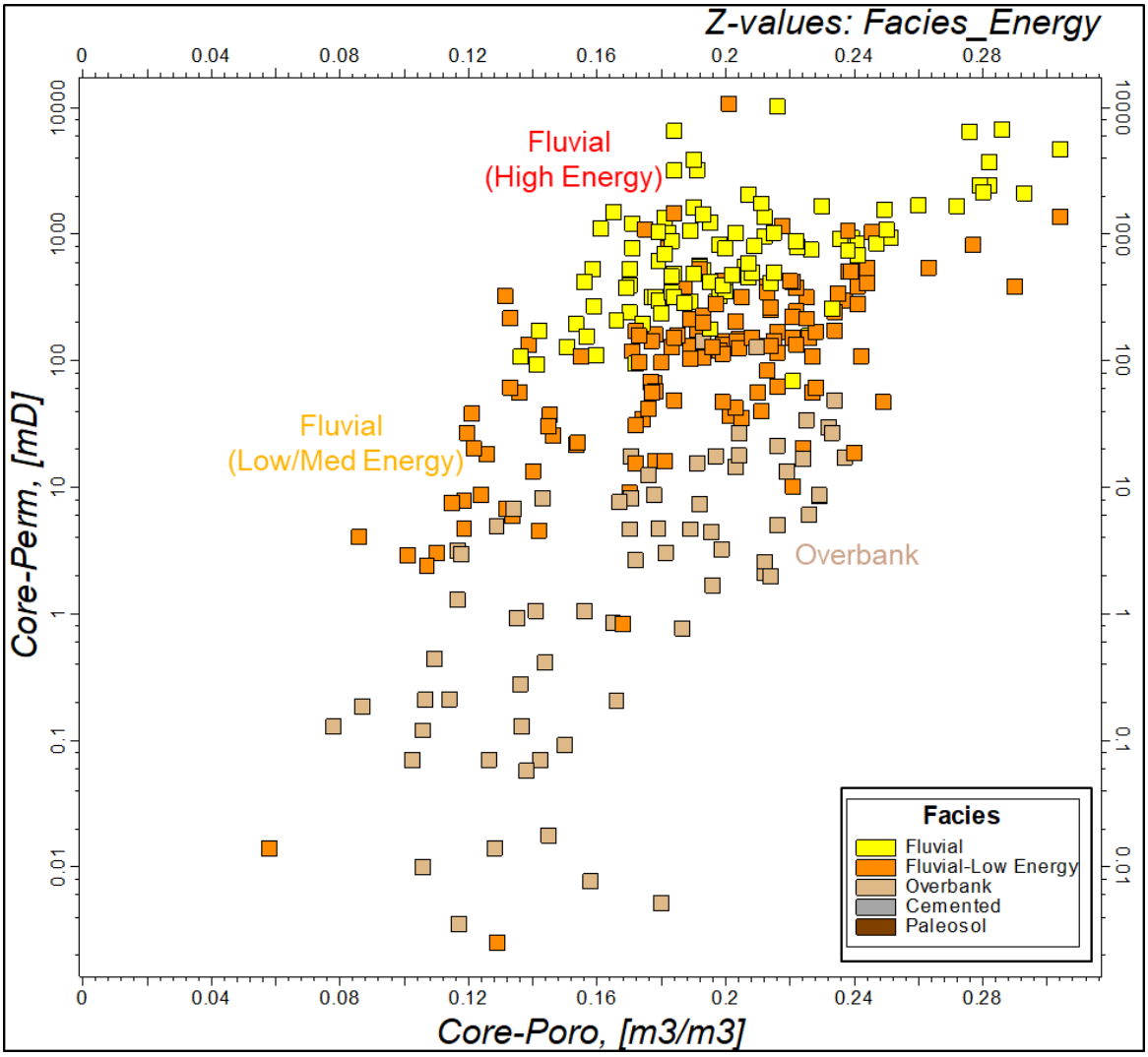



**Figure 3.9: Porosity Permeability By Facies**

## 3.7 Review image log analysis and integrated with seismic

Electrical borehole images were recorded at GSWA Harvey 1 and DMP Harvey 4. Once processed from the raw state to static, (minimum to maximum over the logged interval) and dynamic (moving average) images. It is possible to identify bedding as contrasting layers as well as fractures and faults as conductive features cutting across the well bore and bedding; and in some cases, displacing bedding. It is also possible to identify healed or cemented fractures as highly resistive features cutting across the well bore and bedding. Fractures, both healed and open may also be observed in whole core, however if the core has not been oriented when collected using a special coring system, only the dip of the feature relative to the core axis may be determined. The core information may

be oriented with the aid of borehole images where the feature maybe matched to those seen on the image or in some cases approximately oriented using local stress information. The challenge with using core is that it is often fractured during the coring process.

The fractures interpreted on the image log from GSWA Harvey 1 were displayed on a composite log section, (Figure 3.10 and Figure 3.11). It may be seen that, they are clustered at the top of the Wonnerup member and that there are very few identified over the remainder of the interval. It is noted that, the data does not extend very far into the Yalgorup member. It may also be seen (arrowed) that the group of fractures near the base of the interval occur where there is a slight increase in porosity.

Core from DMP Harvey 2 was described as faulted, however no dip angles were noted. The core was not oriented, but the locations of the fractures are shown in (Figure 3.12). No fractures were noted in the cores from GSWA Harvey 1, DMP Harvey 3 nor DMP Harvey 4 wells. It is suggested that the cores be examined, and the depths of any fractures be recorded, as this information will be useful despite none of the cores being oriented.

The image data from DMP Harvey 4 is limited to the very upper part of the Wonnerup and shows a few events close to the top, see (Figure 3.13).

In conclusion there is probably not enough information form the wells to be able comment further on this issue, however it is possible to model the probability of faults and fractures using a scaling relationship discussed in section 3.10

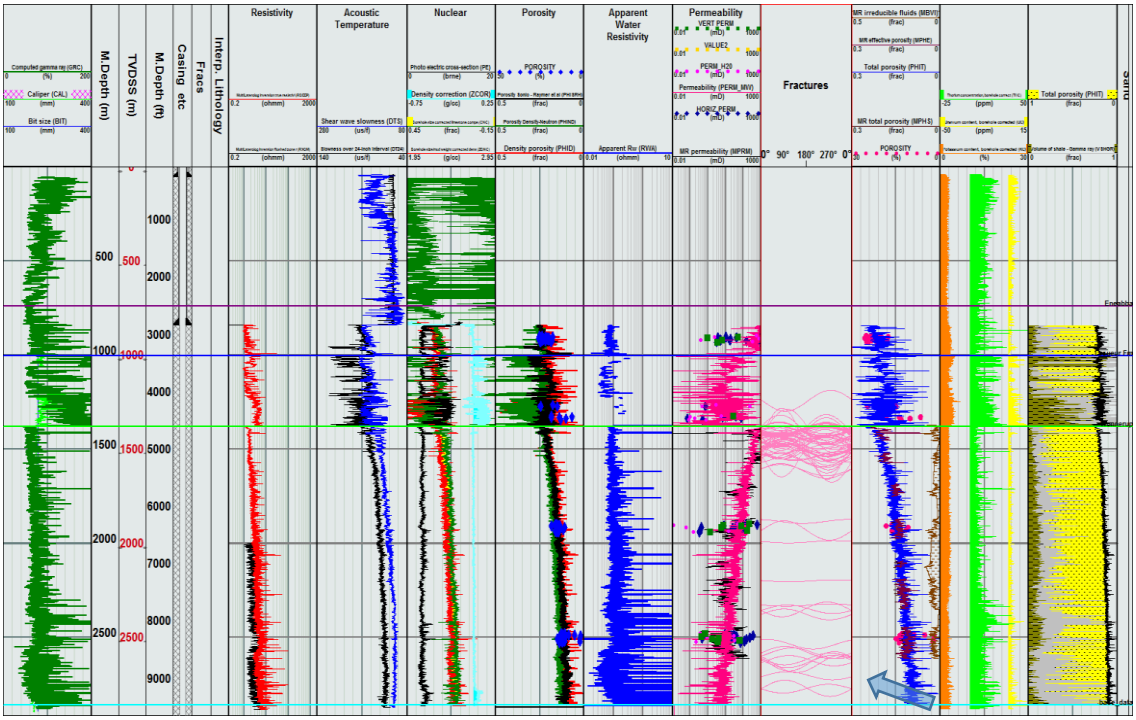



**Figure 3.10: GSWA Harvey 1 Composite Log showing Fractures from Image Log**

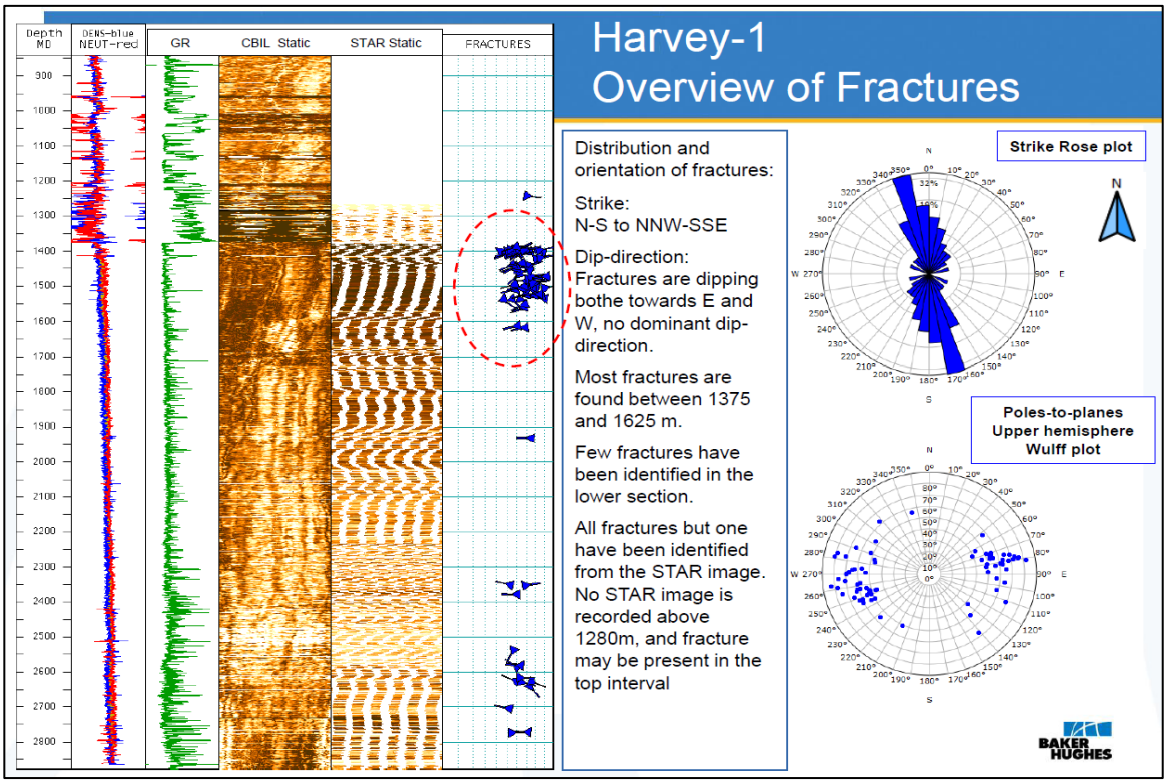



**Figure 3.11: GSWA Harvey 1 Overview of Fractures from Baker Hughes Image Log Study**

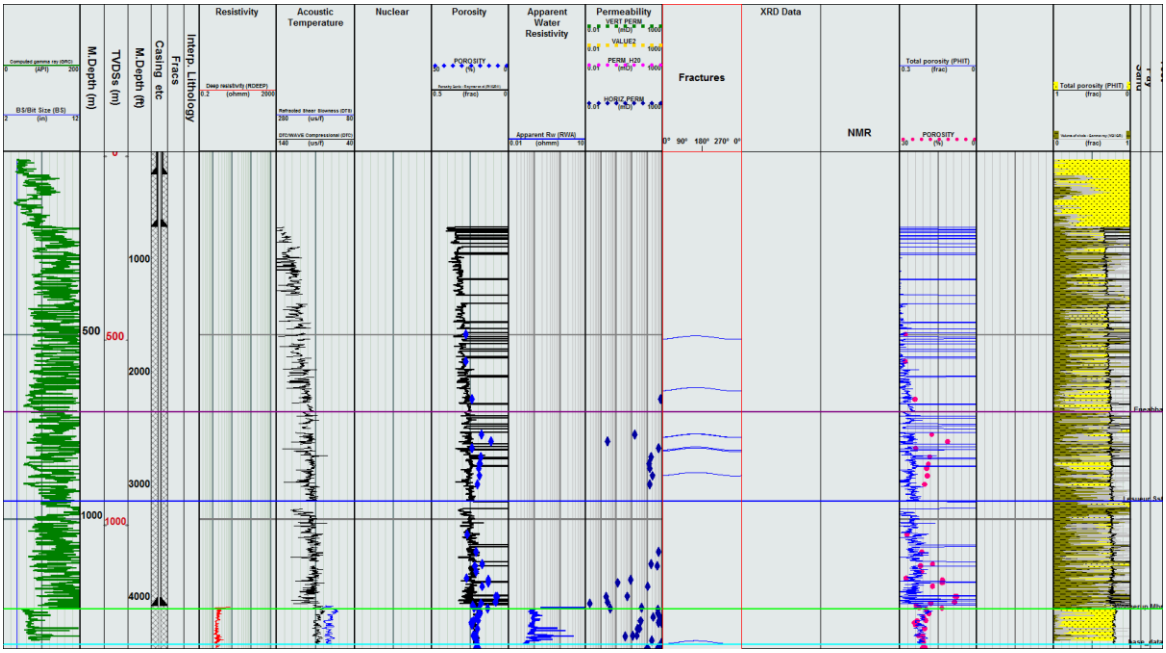



**Figure 3.12: DMP Harvey 2 Composite Log showing Fractures Estimated from Core**

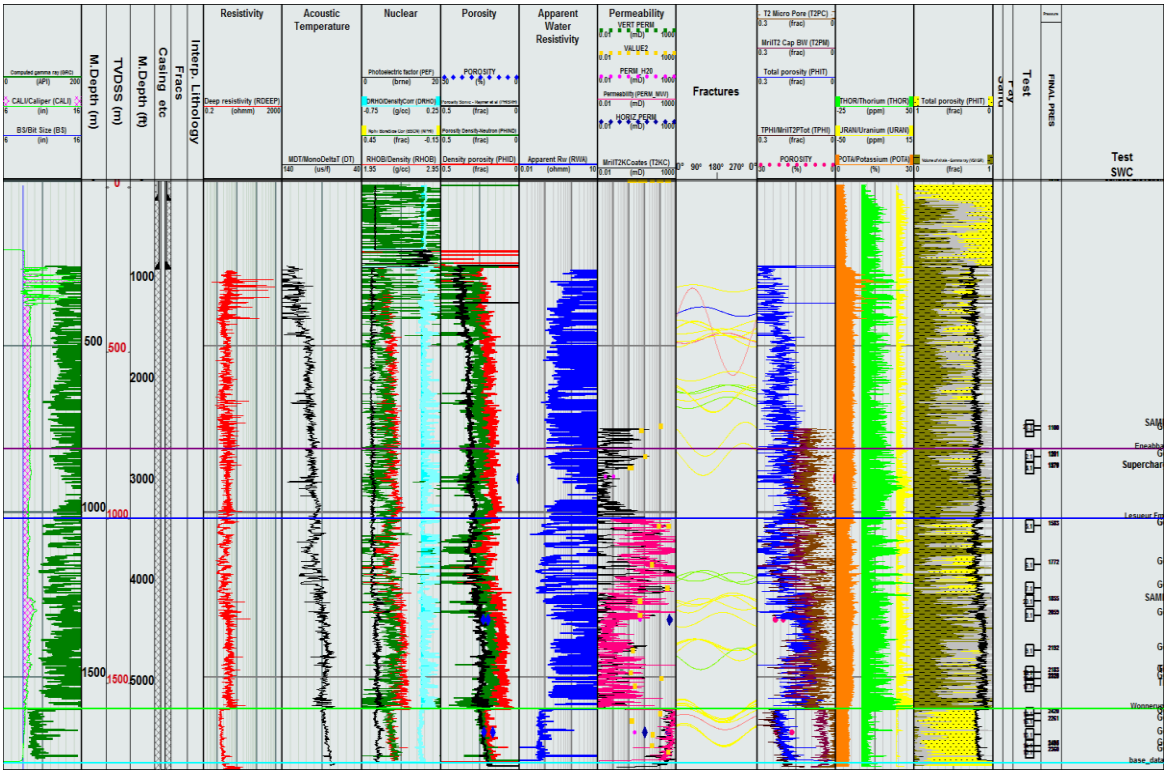



**Figure 3.13: DMP Harvey 4 Composite Log showing Fractures from Image Log**

## 3.8 Analysis of seal quality

The Density-Neutron data was reviewed to determine if it could be used to evaluate seal potential. However, a literature search failed to uncover any use of this technique. When examining seal quality, Mercury Injection Capillary Pressure (MICP) measurements constitute the gold standard. The technique is quick and can be carried out on small samples. It allows an assessment of the process that would cause the breaching of a seal.

As a test, a range of mechanical properties using the Density, Compressional Slowness and Shear Slowness were calculated on the GSWA Harvey 1 data and the MICP results were plotted as points in the far right hand tracks, see (Figure 3.14). It can be seen that over the base of cored section of the Yalgorup member there are many micro pores (purple triangles) and the core did not cover the remaining 25m to the top of the Wonnerup which is mostly claystones associated with the paleosol development. It may also be seen that the computed Unconfined Compressive Strength (UCS) values using

both the Olyer and McNally methods for the Yalgorup vary between 15-45 MPa and that for claystones these values would constitute excellent seal potential as seen in the in the Central North Sea, (Reference 4).

Another approach to provide a quick estimate of the seal potential would be to look at the Transverse Relaxation Time (T2) spectra derived from the NMR tool. Using DMP Harvey 4 as an example. The NMR data shows an abundance of micropores in the Yalgorup in DMP Harvey 4, (Figure 3.15).

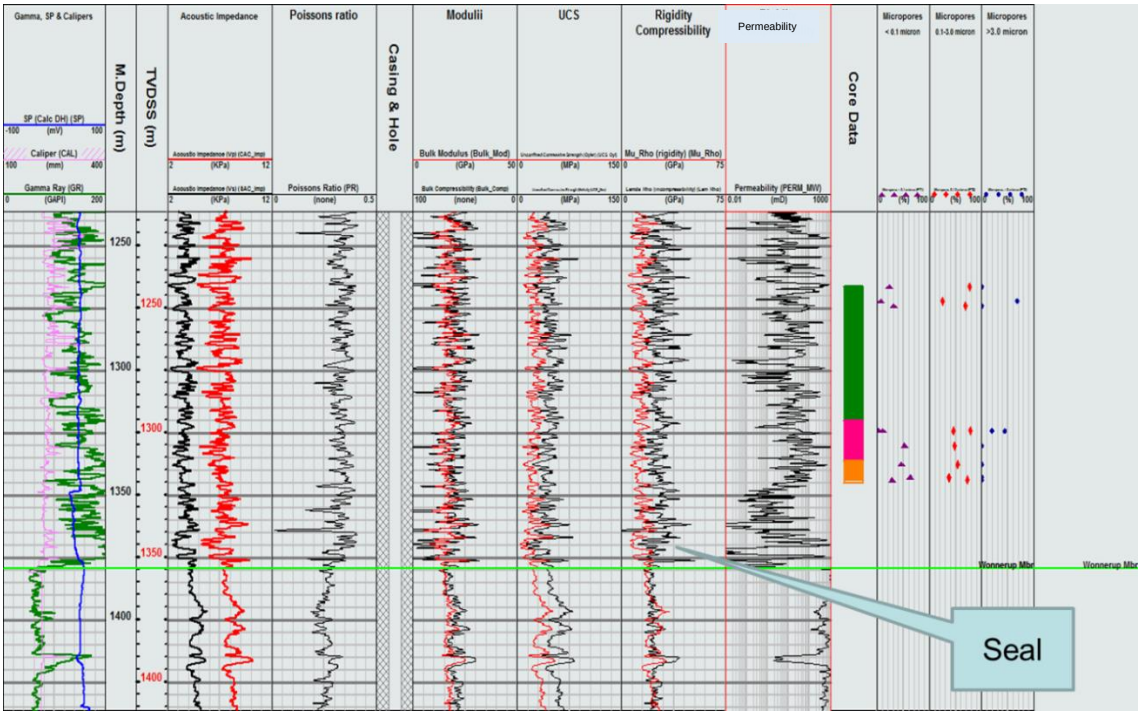



**Figure 3.14: Geomechanical & MICP Data from GSWA Harvey 1**

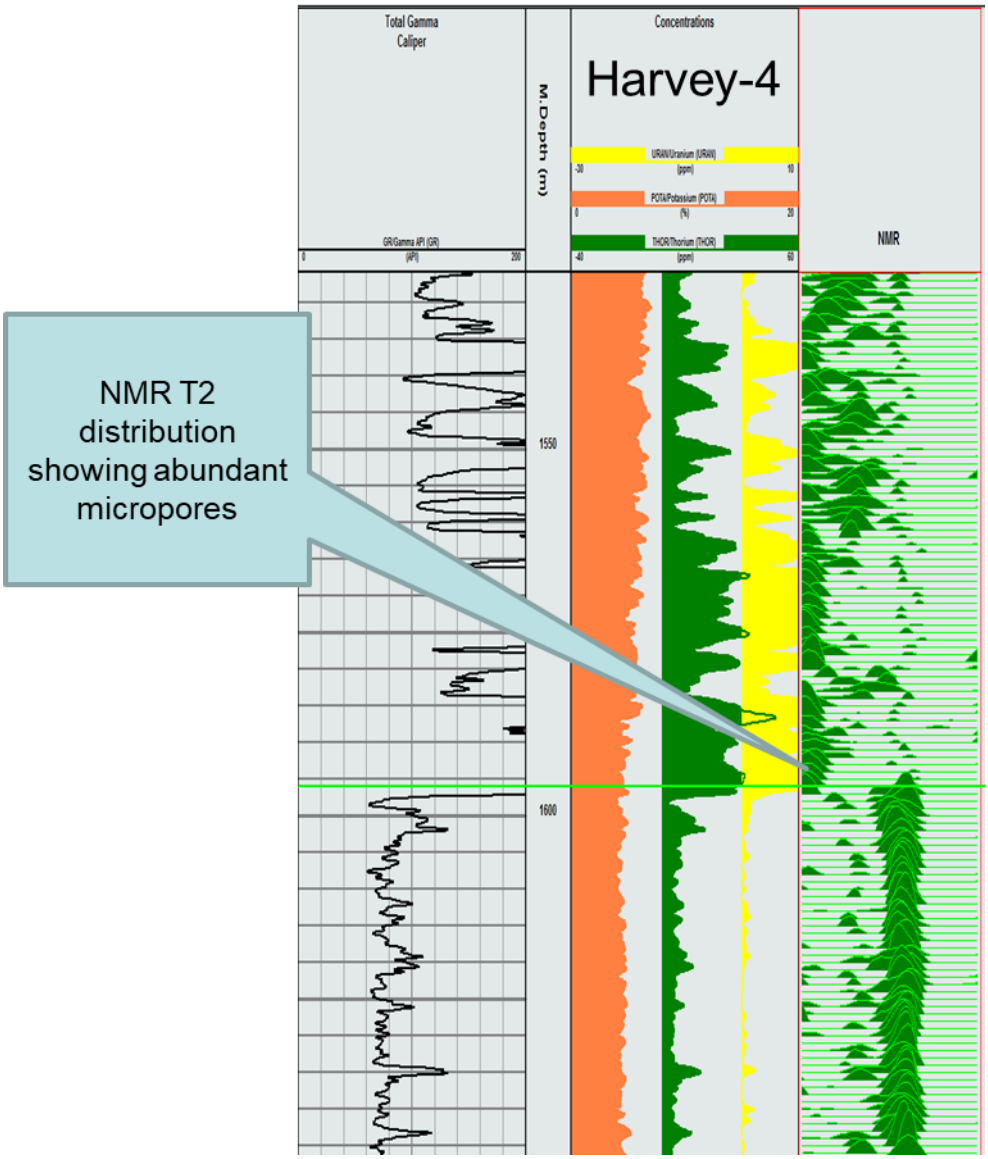



**Figure 3.15: DMP Harvey 4 NMR T2 spectra showing abundant micropores**

## 3.9 Evaluation of Paleosol occurrence

From descriptions of the core taken from the Yalgorup member it is concluded that, many of the claystones are a product of paleosol development due to the presence of rootlets and variably oxidised minerals. It has been observed that, these horizons exhibit quite high concentrations of Thorium and Uranium as recorded by the spectral gamma ray tool see (Figure 3.16). However, only GSWA Harvey 1 and DMP Harvey 4 were logged with the spectral gamma tool.

The geochemistry of Thorium and Uranium indicate very different habitats. The Thorium ion is essentially insoluble, needs a pH of less than three to go into solution to form the soluble $Th(SO_4)^{2+}$ which could be taken up by clay minerals. However, this chemical environment is very remote from a fluvial system. Thorium usually has a detrital habitat existing in heavy minerals such as Monazite (Ce,La,Nd,Th) $PO_4$ or Zircon $ZrSiO_4$ (substituting for Zr) and being concentrated by sedimentary processes such as lag or channel deposits where the dense minerals containing the Thorium resists the flow that sweeps away the lighter minerals such as quartz.

Conversely, the Uranium ion is quite soluble in the pH and Eh conditions found in most ground water but can also be precipitated with minor changes in these conditions. The presence of elevated concentrations of Uranium in groundwater is often an indication of a stagnant system where recharge and groundwater movement is reduced.

The presence of elevated amounts and of Thorium and Uranium seems incompatible with a standard soil.

To further investigate the paleosol, the Hylogger information was examined and not found to be useful as the mineralogical results were not specific enough. The SEM-EDS data provided in the Yalgorup study (Reference 5), shows elevated concentrations of monazite in the red paleosol and saline lake sediments which do not appear to be typical hosts for detrital minerals and it is felt that these results would need some further investigation.

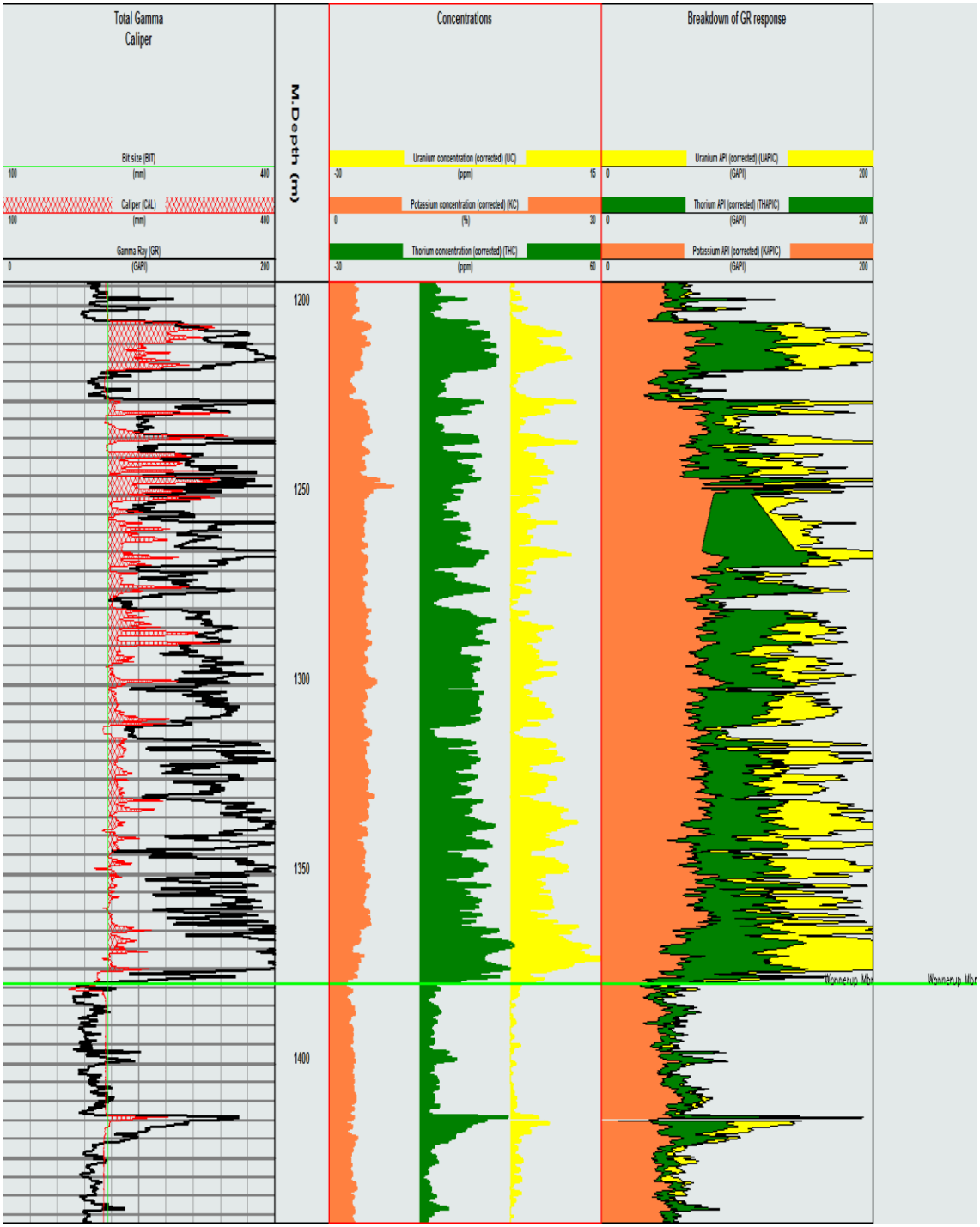



**Figure 3.16: GSWA Harvey 1 Spectral Gamma Ray**

| Depth (m) | 1145.25 | 778.35 | 1027.2 | 1030.8 | 1101.35 | 1386.12 | 717.5 | 888.05 | 1169.35 | 1410.55 |
|---|---|---|---|---|---|---|---|---|---|---|
| Facies | Sand | Paleosol | Red paleosols | Sandy in-fill | Shallow saline lake | Anoxic acid lake | Crevasse splay | Swamp | Swamp | Swamp |
| Minerals | Composition (wt%) | | | | | | | | | |
| Pyrite | 0 | 0 | 0 | 0 | 0 | 0 | 0 | 0.028 | 0 | 0 |
| Berthierine | 0.005 | 0.034 | 0.03 | 0.003 | 0.286 | 0.402 | 0.878 | 0.839 | 0.249 | 0.582 |
| Biotite | 0.026 | 0.047 | 0.238 | 0.059 | 0.165 | 0.248 | 0.046 | 1.284 | 0.823 | 0 |
| Muscovite | 0.089 | 0.003 | 0.041 | 0.049 | 0.049 | 0.054 | 0.012 | 0.1 | 0.352 | 0.042 |
| kaolinite | 0.25 | 0.195 | 0.533 | 0.246 | 0.566 | 1.468 | 1.058 | 5.182 | 9.79 | 35.305 |
| Apatite | 0.001 | 0 | 0.003 | 0 | 0 | 0.006 | 0.004 | 0.074 | 0.001 | 0 |
| Muscovite_Fe | 0.285 | 0.869 | 0.617 | 0.286 | 0.337 | 0.432 | 0.068 | 2.25 | 1.779 | 0.512 |
| Calcite | 0.012 | 0.001 | 0.004 | 0.003 | 0.001 | 1.136 | 0.004 | 0.001 | 0 | 0.026 |
| Chamosite | 0.045 | 0.214 | 0.237 | 0.016 | 0.539 | 7.725 | 1.665 | 1.978 | 1.236 | 0.135 |
| Zircon | 0.01 | 0.005 | 0.023 | 0.008 | 0.05 | 0.063 | 0.016 | 0.013 | 0.03 | 0.003 |
| Ilmenite | 0.179 | 0.031 | 0.067 | 0.042 | 0.166 | 0.324 | 0.063 | 0.07 | 0.127 | 0.009 |
| Rutile | 0.031 | 0.021 | 0.06 | 0.041 | 0.138 | 0.365 | 0.034 | 0.067 | 0.135 | 0.055 |
| Monazite | 0.001 | 0.002 | 0.006 | 0 | 0.007 | 0.004 | 0.001 | 0.002 | 0.003 | 0 |
| Hematite_Magnetite | 0.001 | 0.001 | 0.002 | 0.001 | 0.02 | 0.001 | 0.011 | 0.001 | 0.007 | 0.017 |
| Clinochlore | 0.001 | 0 | 0.015 | 0.001 | 0.002 | 0 | 0 | 0.005 | 0.004 | 0 |
| Hornblende | 0.004 | 0.004 | 0.151 | 0.078 | 0.256 | 0.034 | 0.023 | 0.251 | 0.009 | 0 |
| Clinozoisite | 0.228 | 0.001 | 1.299 | 0.698 | 2.225 | 0.013 | 0.03 | 0.134 | 0.007 | 0.001 |
| Andesine | 0.003 | 0 | 0.027 | 0.034 | 0.084 | 0 | 0.004 | 0.003 | 0 | 0 |
| Anorthite | 0.008 | 0 | 0.006 | 0.002 | 0.001 | 0.004 | 0.009 | 0.001 | 0.004 | 0 |
| Oligoclase | 0.004 | 0 | 0.161 | 0.201 | 0.61 | 0.001 | 0.001 | 0 | 0 | 0 |
| Muscovite-Illite | 0.592 | 1.144 | 1.43 | 0.937 | 0.632 | 0.487 | 1.1 | 0.568 | 1.027 | 0.001 |
| Albite | 0.258 | 0.001 | 4.735 | 7.425 | 11.055 | 0.003 | 0.001 | 0 | 0.001 | 0 |
| Titanite | 0 | 0 | 0.037 | 0.016 | 0.006 | 0 | 0 | 0 | 0 | 0 |

from Bourdet et al, 2017

**Figure 3.17: SEM-EDS data**

Thorium and Uranium are also found in minerals in volcanic ash. It is possible that some of the paleosol's mineralogy will have been derived from distant volcanic eruptions.

The presence of the Uranium the paleosol's above the porous and permeable Wonnerup member would indicate that even a thin claystone in the Yalgorup provides is an efficient long-term seal otherwise the Uranium would have been leached away by fluid movement in the Wonnerup member.

## 3.10 Assess all available data on the Wonnerup

Since the mid 1960's petroleum, exploration wells have been drilled in the southern Perth Basin. In the early years of exploration, exploration wells were subsidised by the Commonwealth Government providing that the exploration company collected specific data, which must include sidewall cores for biostratigraphy, whole core for reservoir property evaluation and wireline logs for evaluation and correlation. This body of data is very useful, with some caveats. The principal caveat being that the core material had to be sent to Bureau of Mineral Resources, Canberra for analysis, and in some cases, these analyses are the only data available for those wells, as some operators did not or could not have the core analysed locally or the results have been lost. In the case of wells drilled in Western Australia in the 1960's it may have taken many weeks or even months to get the core material from the wellsite to the Bureau of Mineral Resources, Canberra for analysis and it would be common for the material to be mechanically and chemically damaged before arrival. These wells include Pinjarra 1, Preston 1 & Wonnerup 1. The core analysis results need to be treated with caution when compared to modern data, or petrophysical results from the log data recorded in the well.

It is noted that towards the base of the Wonnerup member at GSWA Harvey 1 there was a departure from the reduction of porosity with depth trend. This may have been due to fracturing as seen in the borehole images or related to a mineralogical change possibly the preservation of some porosity by the creation of chlorite or some change in depositional environment. Other wells in the region were examined to determine if the porosity degradation with depth was consistent across the region. It is noted that there were some positive departures from a visible porosity decrease with depth trend observable at GSWA Harvey 1, Lake Preston 1 and Sabina River 1 and highlighted in green ellipses, as there were some negative departures from that trend as shown in the (Figure 3.18) and (Figure 3.19).

It should be noted that the trend at Pinjarra 1 is more difficult to observe in the Wonnerup due to only the compressional slowness being available for porosity estimate. Without additional porosity information such as density log, the compressional transit time derived porosity carries a significant uncertainty due to the effects of cementation, coincidently the property under investigation here.

The Raymer et al., slowness transform (Reference 6), has been used to derive porosity can be fine-tuned with some additional data such as density. Trends are similar for GSWA Harvey 1, Lake Preston 1 (13.4km North West) Sabina River 1 (81.9km South), and Pinjarra 1 (35km North), whilst at Wonnerup (76km South and, 6.8km North of Sabina River 1 and Whicher Range 4 (101km South) the trends are different and may indicate different burial histories.

In the region covered by the Harvey wells, there is insufficient data to be able to comment further.

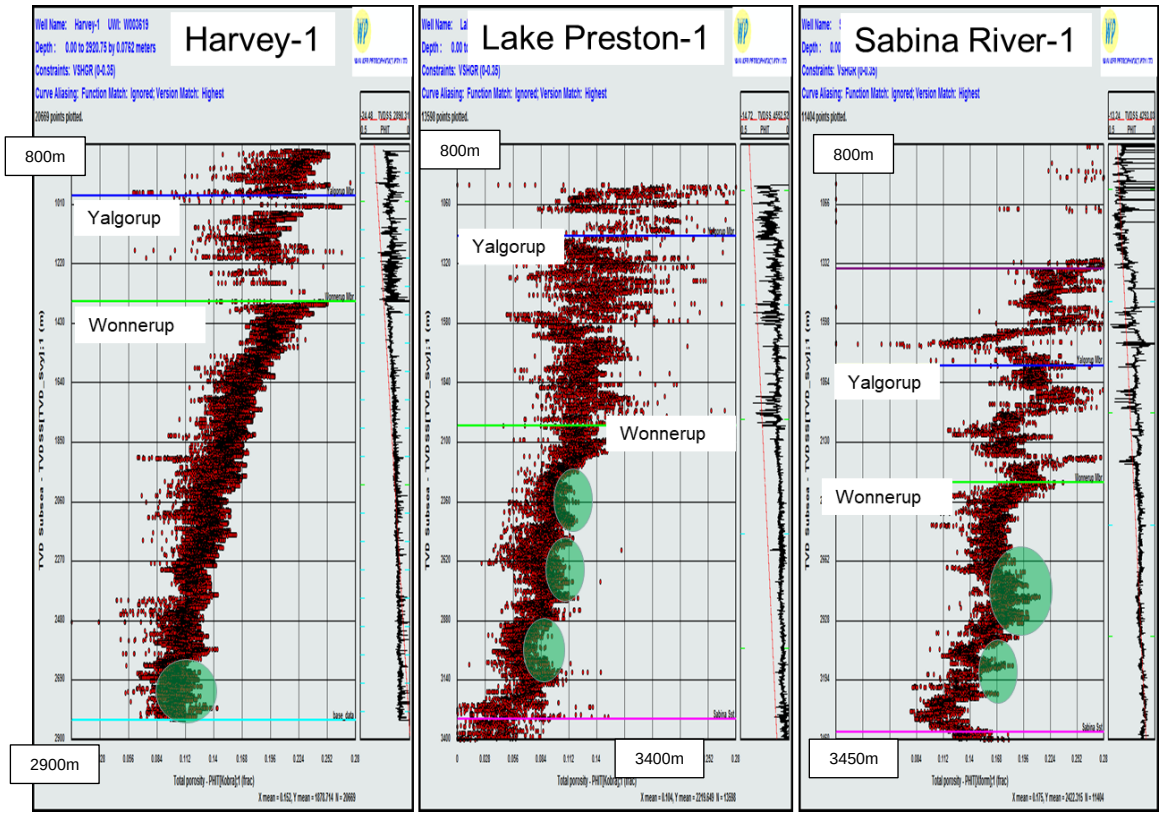



**Figure 3.18: Higher Porosity in lower Wonnerup Member (GSWA Harvey 1, Lake Preston 1, and Sabina River 1)**

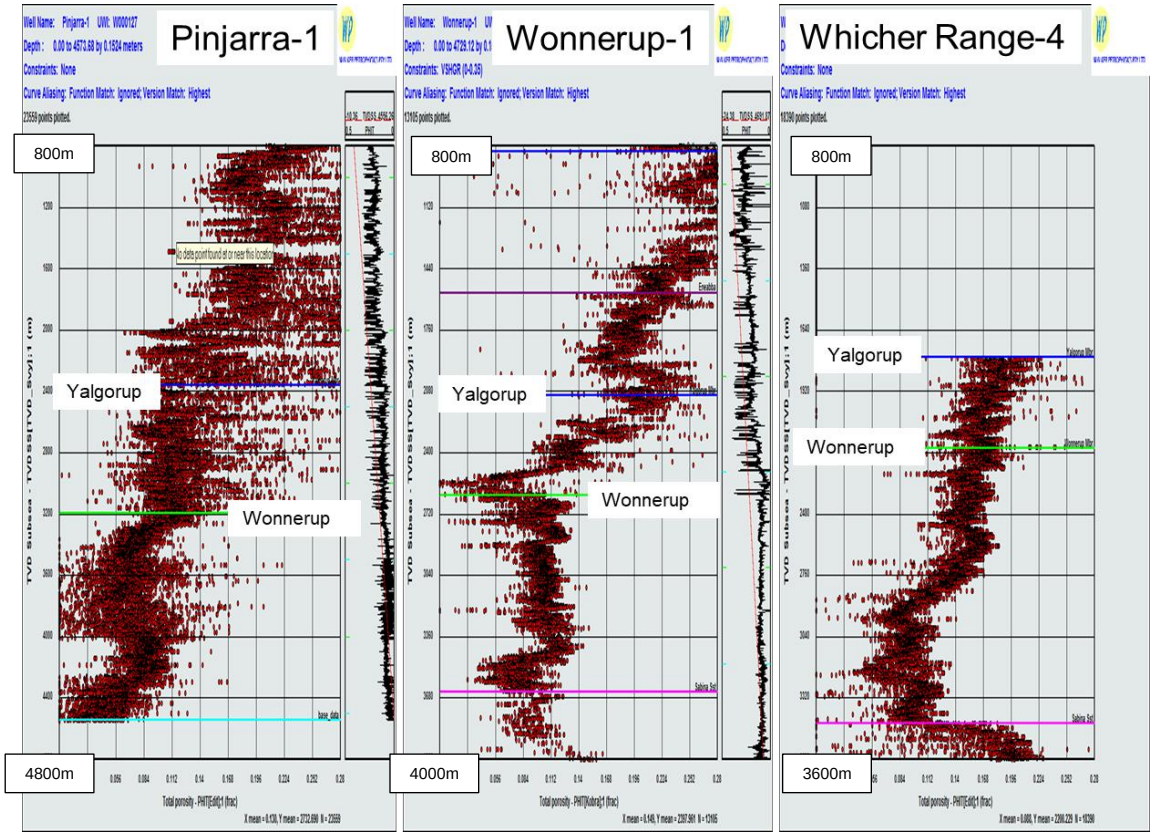



**Figure 3.19: Higher Porosity in lower Wonnerup Member (Pinjarra 1, Wonnerup 1 & Whicher Range 4)**

# 4. REFERENCES


1. Scotese Ancient Earth Atlas (2017), "Plate tectonic maps and Continental drift animations by C. R. Scotese, PALEOMAP Project (www.scotese.com)"

2. Zhan, Y. (2014), 2D Seismic interpretation of the Harvey area, Southern Perth Basin, Western Australia: Geological Survey Western Australia, Record 2014/7

3. Comisky , J. T., K. E. Newsham, J. A. Rushing, T. A. Blasingame, 2007, A comparative study of capillary- pressure-based empirical models for estimating absolute permeability in tight gas sands: 2007 SPE Annual Technical Conference and exhibition, Anaheim, CA, 11-14 November, 2007, SPE 110050.

4. Ingram, G.M., Urai, J.L. & Naylor, M.A., 1997: “Sealing Processes and top seal Assessment.” *In:* Moller-Pedersen, P.& Koestler, A.G. (eds) *Hydrocarbon Seals: Importance for Exploration and Production.* Norwegian Petroleum Society (NPF) Special Publication, Volume **7**, 1997, pp 165-174.

5. Bourdet et al, 2017: Assessment of multi-barrier systems for CO2 containment in the Yalgorup Member, South West Hub. CSIRO report EP174230, June 2017

6. Raymer, L.L., Hunt, E.R., and Gardner, J.S. 1980. An Improved Sonic Transit Time-to-Porosity Transform, paper P. Trans., 1980 Annual Logging Symposium, SPWLA, 1–12.